Paper Sensors Based on Fluorescence Changes of Carbon Nanodots for Optical Detection of Nanomaterials

Evie L. Papadopoulou [1,*], Giulia Biffi [2,3,†], Anitha Senthamizhan [1,‡], Beatriz Martín-García [4,§], Riccardo Carzino [1], Roman Krahne [2] and Athanassia Athanassiou [1,*]

[1] Smart Materials Group, Istituto Italiano di Tecnologia via Morego 30, 16163 Genova, Italy; anitha.senthamizhan@iit.it (A.S.); ricardo.carzino@iit.it (R.C.)
[2] Optoelectronics, Istituto Italiano di Tecnologia via Morego 30, 16163 Genova, Italy; giulia.biffi@iit.it (G.B.); Roman.Krahne@iit.it (R.K.)
[3] Dipartimento di Chimica e Chimica Industriale, Università degli Studi di Genova, via Dodecaneso 31, 16146 Genova, Italy
[4] Graphene Labs Istituto Italiano di Tecnologia via Morego 30, 16163 Genova, Italy; b.martingarcia@nanogune.eu

* Correspondence: paraskevi.papadopoulou@iit.it (E.L.P.); athanassia.athanassiou@iit.it (A.A.)

† Current Address: Materials Physics Center (CFM), Spanish National Research Council (CSIC), 20018 Donostia-San Sebastián, Spain.
‡ Current Address: Nanobiointeractions and Nanodiagnostics, Istituto Italiano di Tecnologia via Morego 30, 16163 Genova, Italy
§ Current Address: CIC nanoGUNE Tolosa Hiribidea, 76, 20018 Donostia, , Spain.

Figure S1: (a) Photoluminescence spectra of carbon dots/PVA water solution at different excitation wavelengths (b) The PL peak of the different systems blueshifts as we move from the carbon dot solution to the PVA/carbon dot solution, to the PVA/carbon dot coated paper, due to stronger localization of the excitons in the presence of a solid matrix. For excitation wavelengths longer than 340 nm, the PL originates from other colour centres (surface states or carbon clusters) and is not affected by exciton localization.

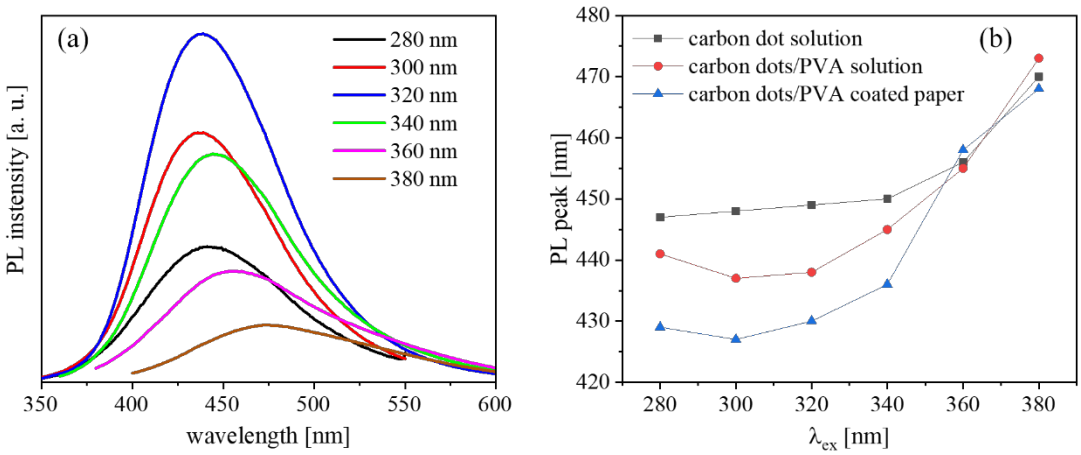

Figure S2: For XPS measurements and in order to measure any possible interaction between carbon dots and silica NPs, we used a simplified system, comprised only of carbon dots and silica NPs deposited on Cu substrate. Cu was used as substrate because XPS, being a technique to study the surface, was not able to detect the interaction of silica NPs and carbon dots when diffused in the cellulose fibres. We have prepared various samples: (i) silica nanoparticles were deposited from the aqueous solution on the Cu substrate and let dry; (ii) carbon dot solution was deposited on Cu substrate and subsequently, when dried, silica NP solution was deposited on top. Samples were left to dry before any measurement. In (a) the Si peak of the pure silica NPs is shown. In (b), we show the Si peaks of silica NPs deposited on carbon dots.

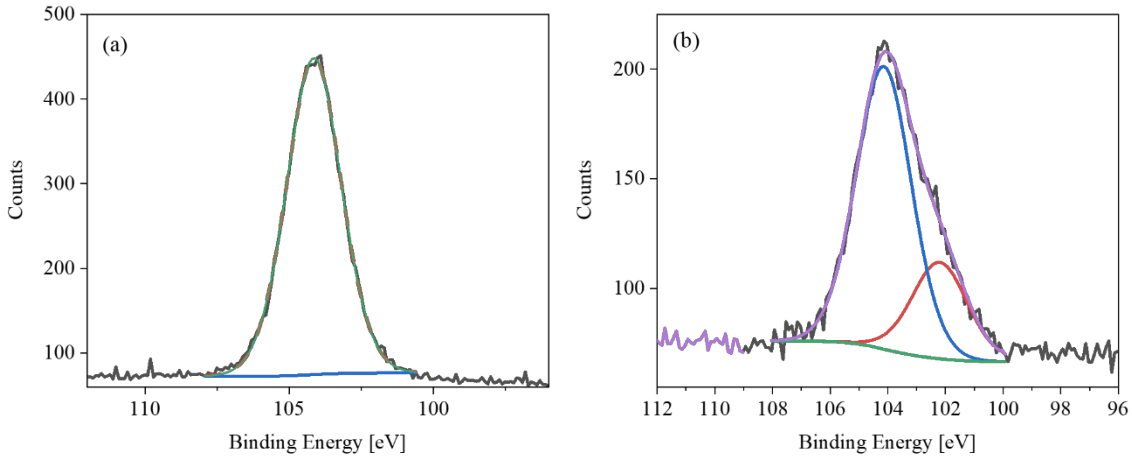

Figure S3: Due to the hydrochromicity of these carbon dots, the role of water in the PL quenching of the paper sensor has been investigated separately. Control experiments were carried out by dipping a paper sensor for 30 s in pure water and measuring PL emission and decay. It then becomes evident that water treatment results in a decrease in the PL intensity (even though all measurements were performed on dry samples). However, the effect of the water treatment is distinctly smaller than that of the silica NPs in the water. In addition, there is no change in the average PL lifetime of the samples that have undergone the control experiments. (a) the PL spectrum is shown for the pristine paper sensor (black line) and after it has been dipped in water (blue line). Further, when the same cellulose sensor is dipped in silica NP solution, the PL emission is further quenched (red line). (b) PL decay curve of paper sensor before and after having been dipped in water. As seen in Figure S3b, there is no significant change in the PL emission decay.

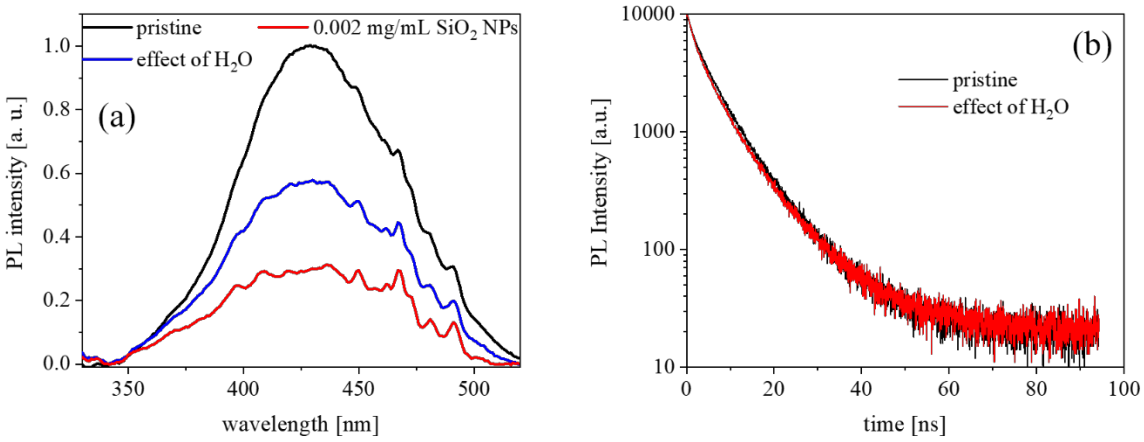

Figure S4: (a) Relative PL and (b) the corresponding average lifetime, with respect the different concentrations of silica aqueous dispersions, for silica concentrations 2×10^{-5} mg/mL to 0.1 mg/mL, in log x-axis. The blue, dashed line indicates the silica concentration where the PL quenches after the paper sensor is exposed to the silica.

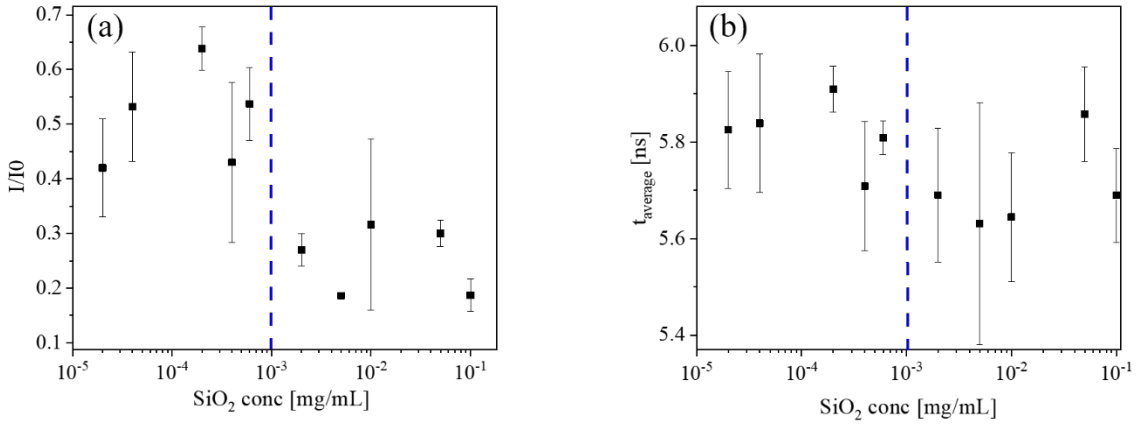

Figure S5: The paper sensors exposed to silica, ZnO and GnP were inspected optically under a UV lamp (254 nm). The fading of the pristine, bright blue photoluminescence after the exposure of the sensors with the target nanomaterial solutions is evident. Exposure of the paper sensor to silica NPs leads to inhomogeneous PL quenching, due to the inhomogeneous diffusion of the silica NPs on the cellulosic fibres. In contrast, ZnO and GnP lead to a homogeneous PL quenching, indicating the homogeneous distribution of these nanomaterials on cellulosic fibres. All paper sensors were exposed to 0.01 mg/mL of the corresponding nanomaterial.

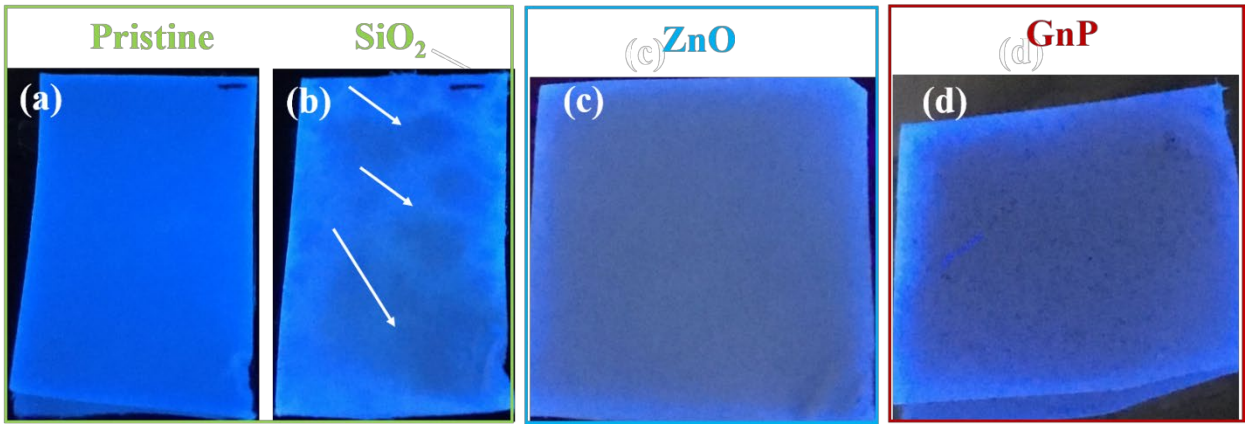

Figure S6: Digital images of paper sensors seen under UV lamp (254 nm) after sweeping a clean surface (upper row) and after sweeping contaminated surfaces (lower row). The same paper strip was used to sweep a clean surface in (a), and subsequently a surface contaminated with 0.2 mg of silica NPs in (d). Similarly, (b) a paper sensor swept over a clean surface and in (e) swept over 0.002 mg of ZnO NPs. Finally, the paper sensor in (c) swept a surface contaminated with 0.001 mg of GnP in (f). The dimensions of the paper strips were ca. 1.0 cm x 1.0 cm.The arrows indicate the areas where the nanomaterials have been deposited, leading to a localized PL quenching.

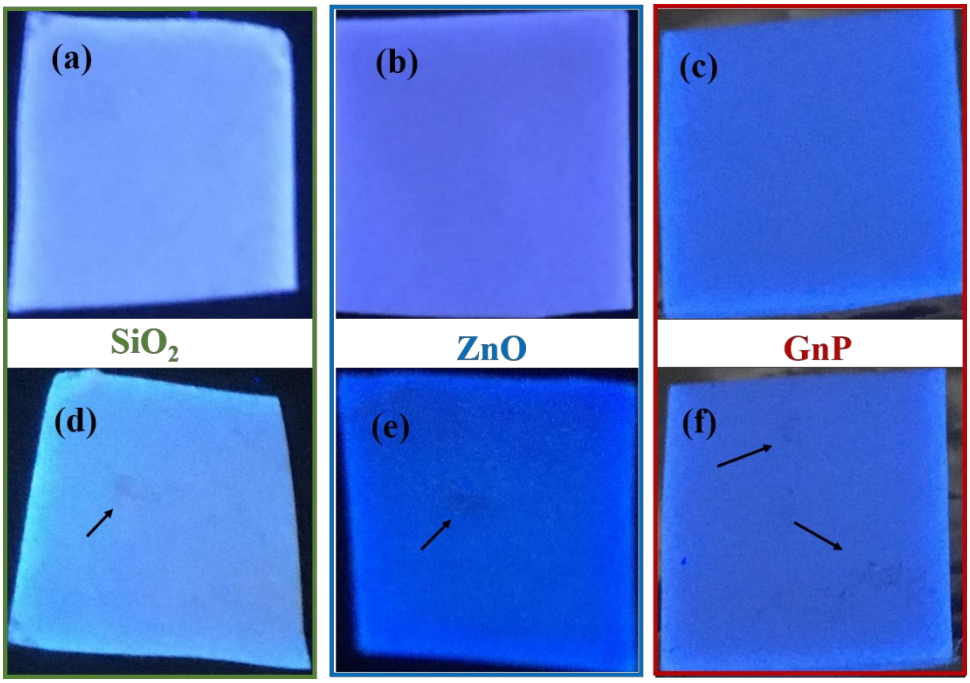

Figure S7: Sweep tests was performed for increasing weight of the different nanopowders. In the following panels, the pristine sample (ca. 1.0 cm x 1.0 cm) is shown, followed by increasing weight of each nanomaterial, for silica NPs (green panel), ZnO NPs (blue panel) and GnP (red panel). The first weight shown for each nanopowder is the lowest weight detectable by the paper sensor. In each panel, the blue images (upper row) correspond to the original photos, while the orange ones (lower row) are the images processed by ImageJ. It is seen, that as the nanopowder weight increases, the colour change corresponding to the local PL quenching becomes more intense.

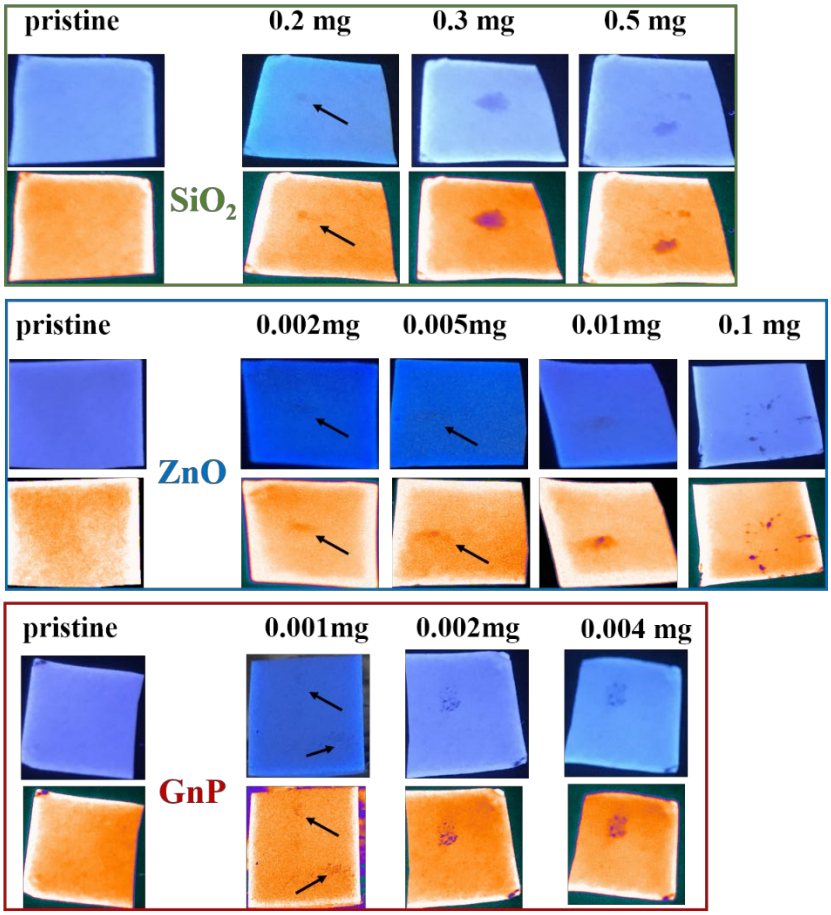

Figure S8: Images of the cellulose sensor performing the sweep test by sweeping the sensor over a dusty windowsill. (a) Pristine sensor (ca. 1.0 cm x 1.0 cm) after sweeping a clean surface, seen under UV lamp (at 254 nm); (b) paper sensor after sweeping the dusty windowsill. (a') and (b') show the same photographs as (a) and (b) respectively, after they have been processed with ImageJ to enhance the colour differences. Inspection of the images does not reveal any PL quenching due to the presence of dust.

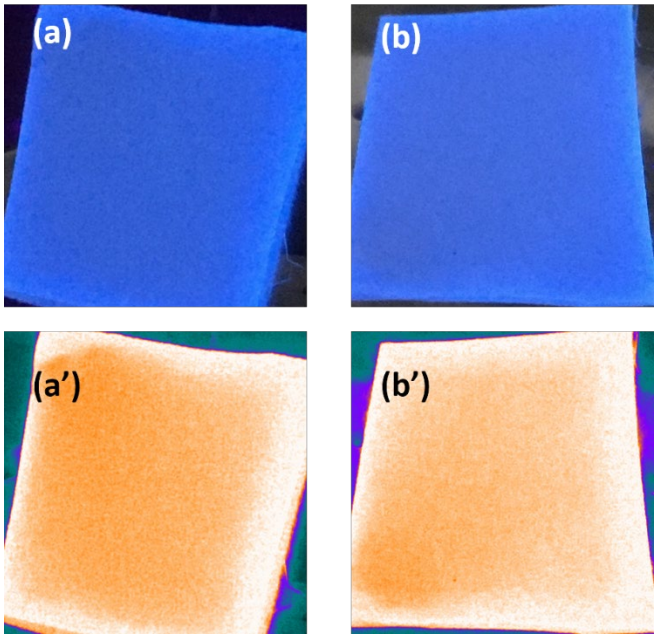

Table S1: The average lifetimes were calculated using the following equation for bi-exponential decay fitting:

$$\tau_{average} = \frac{A_1\tau_1^2 + A_2\tau_2^2}{A_1\tau_1 + A_2\tau_2}$$

where τ_i are the decay times and Ai represent the amplitudes of the components1. Fitting parameters for carbon dot/PVA solution and carbon dot/PVA coated paper.

sample	τ1 [ns]	A1	τ2 [ns]	A2	$\tau_{average}$ [ns]
Carbon dots/PVA solution	2.88	0.506	9.63	0.437	7.70
Carbon dots/PVA coated paper	2.15	0.403	6.97	0.619	6.13

sample	τ0 [ns]	A0	τ1 [ns]	A1	τ2 [ns]	A2	$\tau_{average}$ [ns]
Carbon dots/PVA coated paper	-	-	2.15	0.403	6.97	0.619	6.13
+0.0001 mg/mL ZnO	1.66	0.530	5.65	0.467	13.31	0.050	6.03
+0.01 mg/mL ZnO	1.59	0.555	5.62	0.448	13.55	0.047	5.99

Table S3: Fitting parameters for paper sensor exposed to silica NPs.

sample	τ1 [ns]	A1	τ2 [ns]	A2	$\tau_{average}$ [ns]
Carbon dot/PVA coated paper	2.15	0.403	6.97	0.619	6.13
+0.0002 mg/mL SiO_2	2.08	0.479	6.87	0.561	5.88
+0.002 mg/mL SiO_2	1.89	0.470	6.72	0.55	5.78
+0.01mg/mL SiO_2	2.00	0.655	7.21	0.396	5.57
+0.1 mg/mL	2.00	0.639	7.17	0.406	5.59